Desalination and Water Treatment
www.deswater.com

doi: 10.5004/dwt.2018.22115

109 (2018) 297–306
March

Continuous flow column adsorption of mordenite zeolite–polymer composite fibers for lead removal

Kohtaroh Nakamoto[a], Masaru Ohshiro[b], Takaomi Kobayashi[a,*]

[a]*Department of Materials Science and Technology, Nagaoka University of Technology, 1603-1 Kamitomioka, Nagaoka, Niigata, Japan, Tel. +81 258 47 9326; Fax: +81 258 47 9300; emails: takaomi@vos.nagaokaut.ac.jp (T. Kobayashi), kotaro_nakamoto@mst.nagaokaut.ac.jp (K. Nakamoto)*
[b]*Kasai Corporation, 578-3 Kawaguchi Akiha, Niigata, Japan, Tel. +81 250 24 3900; Fax: +81 250 24 4100; email: ohshiro@kasai-corporation.co.jp*

Received 28 November 2017; Accepted 26 February 2018

ABSTRACT

A fibrous composite adsorbent fabricated by wet phase inversion, mordenite zeolite–polymer composite fiber, was investigated using column adsorption experiments. Lead ion adsorption with the composite fiber was examined at various volumetric flow rates, column heights, initial concentrations of Pb^{2+}, and solution pH. Experiment results revealed that increasing flow rate and decreasing column height led to lower adsorption capacities of the Pb^{2+} ion because of the short residence time. Furthermore, higher initial concentration at 0.1–0.2 mM and lower pH led to lower adsorptivity capacities because the initial Pb^{2+} concentration and solution pH adversely affected the column adsorption performance. Results show that the Adams–Bohart and Yoon–Nelson models fitted the experimental breakthrough curves well. For a quaternary mixed solution containing Pb^{2+}, Cd^{2+}, Cu^{2+}, and Ni^{2+}, packed column adsorption of the fibrous composite adsorbent showed that Pb^{2+} was adsorbed selectively, leading to predominant removal of Pb^{2+} because Cu^{2+} and Ni^{2+} were desorbed by the column operation.

Keywords: Column adsorption; Fibrous adsorbent; Lead removal; Mordenite zeolite; Polymer composite

1. Introduction

Concern has arisen in recent decades about environmental water pollution by heavy metals. Increasing concentrations of heavy metals including lead, cadmium, copper, and nickel cause harmful effects such as anemia, organ failure, and neurological damage [1,2]. Therefore, laws to protect water quality have been enacted, mandating that concentrations of heavy metals in the environment meet legal standards to decrease grave risk [3]. Nevertheless, people in some countries are still exposed to heavy metal pollution because of mining development [4], plating factory effluents [5], and manufactured products [6,7]. These anthropogenic sources of heavy metals lead to environmental accumulation in water system sediments. When circumstances related to polluted sediments arise as the result of engineering works and natural disasters such as dredging operations and flood events, the accumulated heavy metals might be released to water systems [8]. Such releases of large amounts over a short period increase the risk of exposure to heavy metals to the human body through drinking water, plants, and aquatic organisms.

Consequently, purification process including membrane filtration [9], chemical precipitation [10], and adsorption [11] has been used to remove heavy metals from water. Among these purification techniques, adsorption is a simple and effective method. Examples of widely used adsorbents are activated carbon [12], clay minerals [13], iron oxide [14], mesoporous silica [15], and zeolite [16]. Especially, zeolite takes priority for inexpensive and high-performance heavy metal removal processes. Zeolite is known to be a naturally occurring aluminosilicate and to have a large surface area because of its regular porous and three-dimensional structure

* Corresponding author.

consisting of silicate, oxygen and aluminum atoms [17]. Zeolite has many applications such as catalysis [18], building materials [19], and soil remediation [20]. In addition, the zeolite contains cations such as Na^+, K^+, and Ca^{2+} for charge compensation at its negative charge site. Consequently, positively charged ions can be replaced with other cations, so the zeolite has the removability of heavy metals such as Pb^{2+} and Cd^{2+}. For this specific characteristic of zeolite, the removability and selectivity of heavy metal ions have been studied [21,22].

However, for practical water treatment applications, zeolite is unsuitable even though the adsorbent has several benefits. One of the reasons is that the powder zeolites cannot be easily collected from water because they are fine powder. Granular zeolite overcomes this shortcoming, but the adsorption ability of the granule is less than that of powdered zeolite in practical uses [23]. In addition, when the column operation with the zeolite granules is used for removal of heavy metal ions in continuity, high pressure and low treatment efficiency disturbed operation. Consequently, adsorbents for removal of heavy metals with high handleability, high adsorption ability, and high permeability are indispensable. In our earlier work, fabricating mordenite zeolite–polymer composite fiber was reported for decontamination of radioactive Cs [24]. Because this composite fiber has sponge-like structure with zeolite particles supported on polymer scaffold (Fig. 1), the porous structure and fibrous shape readily give effective benefits to each contaminant. In addition, better handling and high permeability of this waste medium through its use inside fiber adsorbent are merits. Moreover, the adsorption behavior of Pb^{2+}, Cd^{2+}, Cu^{2+}, and Ni^{2+} has been investigated as composite fiber adsorbents [25] for the effective treatment of organic dye waste [26]. Results revealed that adsorption of each contaminant such as heavy metal ions occurred in a monolayer adsorption system because it obeyed the Langmuir adsorption isotherm. Among heavy metal ions, the composite fibers promise to eliminate Pb^{2+} by the adsorbent. However, in practical terms, operation column separation is useful for the continuous treatment of such polluted water. Although it is important to ascertain the performance of such fibrous adsorbents, little is known about the dynamic adsorption behavior of heavy metals by composite fiber adsorbents in column separation mode. Given this research background, the present investigation elucidates the dynamic adsorption behavior of Pb^{2+} for a continuous flow column system. Therefore, the dynamic adsorption behavior of the composite fibers was investigated first when packing them was performed in the column. Then, the adsorption tests were conducted in a mixed solution, when flow into the column was compared with those of other ions: Cd^{2+}, Cu^{2+}, and Ni^{2+}.

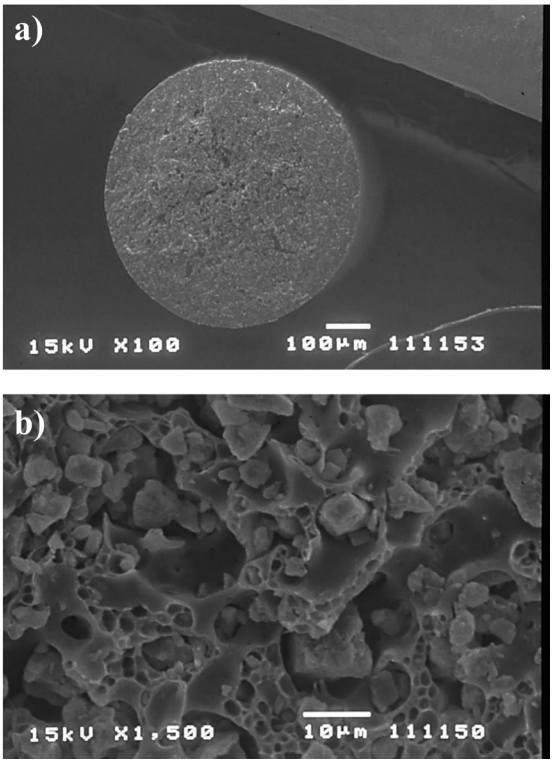

Fig. 1. SEM micrographs of zeolite–polymer composite fibers: (a) ×100 and (b) ×1,500.

2. Experimental setup

2.1. Materials

Polyether sulfone (PES, Ultrason E 2010) was obtained from BASF Co. Ltd. (Germany); *N*-methyl-2-pyrrolidone (NMP) was purchased from Nacalai Tesque Inc. (Japan). Natural mordenite zeolite powder was purchased from Nitto Funka Trading Co., Ltd., Japan. Working aqueous solutions of Pb^{2+}, Cd^{2+}, Cu^{2+}, and Ni^{2+} were prepared from heavy metal stock solutions containing 0.1 M nitrate salt of heavy metals. In addition, 69 wt% of nitric acid (Wako Pure Chemical Industries Ltd.) was used for adjustment of the solution pH.

2.2. Preparation of mordenite zeolite–polymer composite fiber

Mordenite zeolite–polymer composite fiber was fabricated by wet phase inversion technique. Details of processes are reported in our previous study [24]. The composite fiber for all adsorption tests contain 58.8 wt% of mordenite zeolite. An investigation of characteristic and adsorption properties of heavy metals (Pb^{2+}, Cd^{2+}, Cu^{2+}, and Ni^{2+}) for the composite fiber was conducted in our earlier study [25].

2.3. Adsorption experiment

For adsorption experiments in a column flow system, a polyvinyl chloride cylindrical tube with 15–30 cm height and a 2 cm inner diameter was used for packing 15–30 g of zeolite–polymer composite fibers that had been cut to 20 cm length. In the column experiment for Pb^{2+}, the flow rate, column height, initial Pb^{2+} concentration, and solution pH were changed as presented in Table 1. The 0.05–0.2 mM Pb^{2+} feed solution was flowed continuously into the packed column in the up direction using the tubing pump (Master flex) at a 5–15 cm^3/min of flow rate. Effluent samples were collected from the top of the columns at different times. In addition, for the separation study in mixed heavy metal solution, 20 g of the composite fiber was packed in the 20 cm length column. Then 0.05 mM quaternary heavy metal (Pb^{2+}, Cd^{2+}, Cu^{2+}, and Ni^{2+}) at pH 5 was flowed into the column at a 10 mL/min of flow rate.

Table 1
Column condition and parameter of breakthrough curves

Column height H (cm)	Mass of packed composite fiber M (g)	Flow rate v (mL/min)	Initial concentration C_o (mmol/L)	pH	Empty bed residence time, EBRT (min)	t_b (h)	Bed volume, BV_b	t_{st} (h)	Height of unused bed, H_{UNB} (cm)	q_m (mmol/g)
20	20	5	0.2	5	12.56	43	360	142	13.9	0.257
20	20	10	0.2	5	6.28	10	168	74	17.3	0.241
20	20	15	0.2	5	4.19	4	101	58	18.6	0.221
30	30	10	0.2	5	9.42	22	246	120	24.5	0.252
15	15	10	0.2	5	4.71	4	89	62	14.0	0.229
20	20	10	0.15	5	6.28	20	335	127	16.9	0.297
20	20	10	0.1	5	6.28	33	553	187	16.5	0.326
20	20	10	0.05	5	6.28	116	1,944	318	12.7	0.321
20	20	10	0.2	3	6.28	–	–	55	–	0.134
20	20	10	0.2	2	6.28	–	–	26	–	0.032

The effluent concentrations of heavy metals were sampled and determined using atomic adsorption spectroscopy (AAS, AA-6300; Shimadzu Corp., Japan) with 217.0, 228.8, 324.8, and 232.0 nm atomic lines for Pb^{2+}, Cd^{2+}, Cu^{2+}, and Ni^{2+}. After measurements were taken five times for each sample, average measurement values were provided to the results. The standard deviation was also calculated to ascertain the error range from average values. For every condition, the standard deviation was within about 0.01. Consequently, it is believed that the variation was not significant and the measurement values were valid. The column adsorption performance is usually described by the breakthrough curve. The breakthrough curve is expressed as a plot of C_t/C_o and vs. t in this study, where C_t is the effluent heavy metal concentration (mM), C_o represents the initial heavy metal concentration (mM), and t denotes time (h). The saturation adsorption amount q_m (mmol/g) was calculated using the following equation:

$$q_m = \frac{v}{1000M}\int_{t=0}^{t=t_{st}} \left(C_o - C_t\right)dt \tag{1}$$

In that equation, v represents the flow rate (cm^3/h), M stands for the mass of zeolite in packed composite fibers (g), and t_{st} denotes the time at saturation point ($C_t/C_o = 0.95$).

The empty bed residence time (EBRT) (min) was calculated using the following equation [27]:

$$\text{EBRT} = \frac{\pi r^2 H}{v} \tag{2}$$

Therein π is the circle ratio, r denotes the column radius (cm), and H is the column height.

To evaluate the total volume of treated water for the volume of the composite fibers, the bed volume at breakpoint (BV_b) was obtained. BV_b is defined by the following equation [28]:

$$\text{BV}_b = \frac{60vt_b}{\pi r^2 HV_o} \tag{3}$$

In that equation, t_b represents the time at breakpoint ($C_t/C_o = 0.1$). V_o is the packing ratio of the fiber inside column. In all experiment cases, V_o was 57 vol%.

Height of the unused bed (H_{UNB}) (cm) is [29]:

$$H_{\text{UNB}} = \left(1 - \frac{t_b}{t_{st}}\right)H \tag{4}$$

where H_{UNB} represents the mass transfer zone, which is an indication for diagnosing better column adsorption performance [30]. When the value of H_{UNB} is small, a narrow mass transfer zone and steep breakthrough curve occur [29]. For better column operations, a small value of H_{UNB} is required [30].

The adsorption selectivity of heavy metals for the composite fibers in quaternary mixed heavy metal ion was investigated in terms of separation factor α, which is defined as:

$$\alpha = \frac{Y_a / Y_b}{X_a / X_b} \tag{5}$$

where Y_a and X_a are the mole fractions of feed and eluting solutions, respectively, for target metal ions. Also, Y_b and X_b are the mole fractions of feed and eluting solutions, respectively, for every metal ion excluding the target metal ion.

2.4. Dynamic adsorption models

Three adsorption models were applied to fit experimental breakthrough curves: the Adams–Bohart model, Wolborska model, and Yoon–Nelson model. The Adams–Bohart model is the assumption model considered for a rectangular isotherm. The influence rate of adsorption is proportional to both the concentration of the adsorbing species and the residual capacity of the adsorbent [31,32].

$$\frac{C_t}{C_o} = \frac{1}{1+\exp\left(k_{AB}N_o\frac{H}{L_V} - k_{AB}C_o t\right)} \quad (6)$$

where k_{AB} is the kinetic constant of the Adams–Bohart model (L/mmol h), N_o represents the adsorption capacity per unit volume of the bed (mmol/L), and L_v denotes the linear velocity (cm/h). The maximum adsorption capacities per adsorbent mass q_{AB} (mmol/g) are calculated using following equation:

$$q_{AB} = \frac{N_o \pi r^2 H}{1000M} \quad (7)$$

The Wolborska model is a simplified adsorption representation that emphasizes the general mass transfer for the diffusion mechanism for a low concentration range only for the breakthrough curve. The equation is expressed as [33]:

$$\frac{C_t}{C_o} = \exp\left(\frac{\beta C_o t}{N_o} - \frac{\beta H}{L_V}\right) \quad (8)$$

where β is the kinetics coefficient of the external mass transfer (h^{-1}).

In addition, the maximum adsorption capacity q_w (mmol/g) is obtainable from the following equation, identically to q_{AB}:

$$q_w = \frac{N_o \pi r^2 H}{1000M} \quad (9)$$

Moreover, the Yoon–Nelson model is applied. As shown in the empirical model with simpler model equation expressed as [34]:

$$\frac{C_t}{C_o} = \frac{1}{1+\exp(k_{YN}(\tau - t))} \quad (10)$$

where k_{YN} is the Yoon–Nelson constant (h^{-1}) and τ is time (h) at 0.5 of C_t/C_o.

These models were fitted for the results of column breakthrough curves. The parameters of these three experimentally applied models were analyzed using nonlinear regression with software (Origin version 8.5).

3. Results and discussion

3.1. Column decontamination of Pb^{2+} by the composite fiber adsorbents

Breakthrough curves of Pb^{2+} for the composite fibers in difference column parameters are presented in Figs. 2–5. In addition, Figs. 2–5 predicted curves shown by the Adams–Bohart model, Wolborska model, and Yoon–Nelson model as shown, respectively, with the solid line, dotted line, and broken line. The results and discussion related to these models are presented in section 3.2.

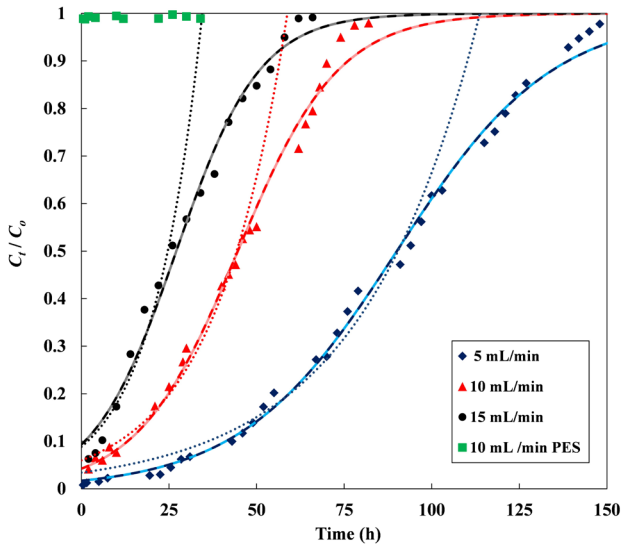

Fig. 2. Breakthrough curves of Pb^{2+} at different volumetric flow rates (— Adams–Bohart model, ··· Wolborska model, and -- Yoon–Nelson model).

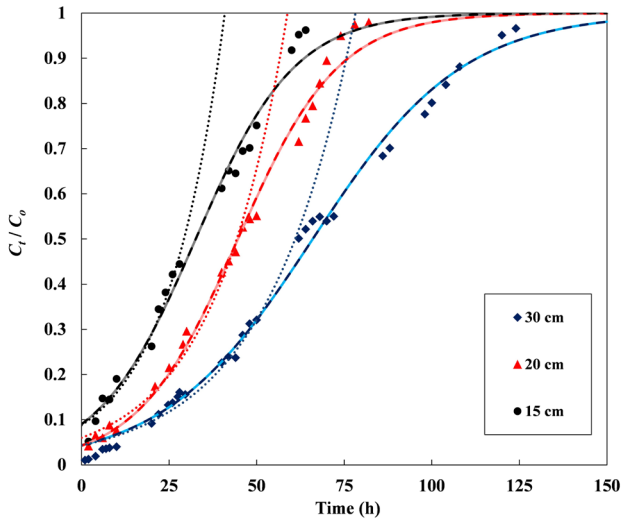

Fig. 3. Breakthrough curves of Pb^{2+} at different column height (— Adams–Bohart model, ··· Wolborska model, and -- Yoon–Nelson model).

Column adsorption of Pb^{2+} aqueous solution was studied using 20 cm height and 2 cm diameter of the column, when 20 g of the composite fibers was packed. Here, 0.2 mM of Pb^{2+} aqueous solution was flowed at 5, 10, and 15 cm^3/min. The obtained breakthrough curves of the Pb^{2+} removal at each flow rate are presented in Fig. 2. It is readily apparent that values of C_t/C_o rise slowly with time. As presented in Table 1, increasing empty bed residence time (EBRT) was observed with a decreasing flow rate. For the breakpoint defined as C_t/C_o = 0.1 in the breakthrough curve, the break times (t_b) for 5, 10, and 15 cm^3/min were, respectively, 43, 10, and 4 h. The bed volumes (BV_b) were, respectively, 360, 168, and 101. Results show that the slow flow rate provided a long break time and the composite fiber much volume of treated

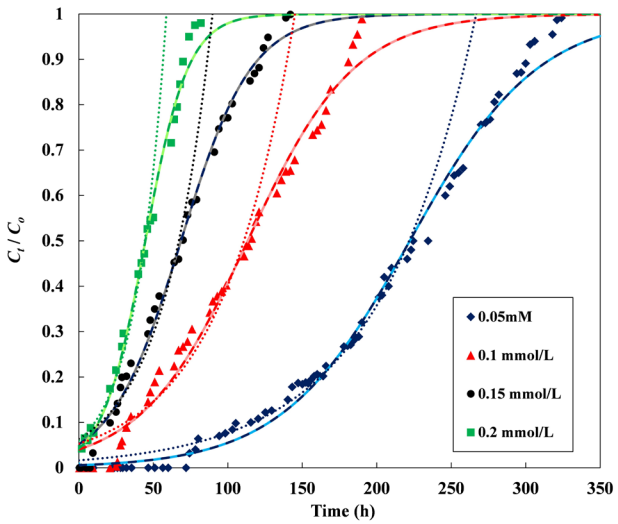

Fig. 4. Breakthrough curves of Pb^{2+} at different initial Pb^{2+} concentration (— Adams–Bohart model, ··· Wolborska model, and -- Yoon–Nelson model).

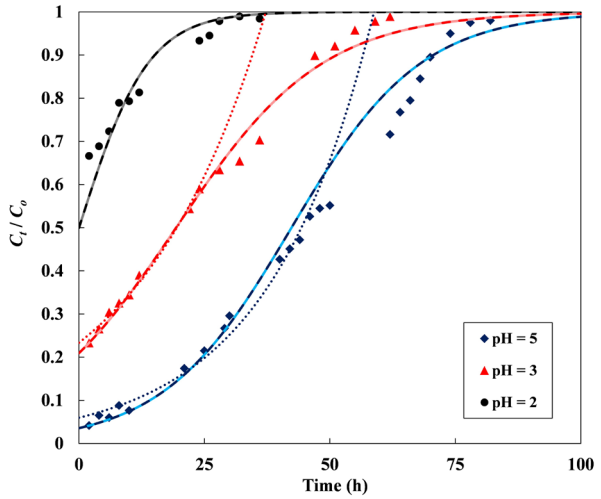

Fig. 5. Breakthrough curves of Pb^{2+} at different solution pH (— Adams–Bohart model, ··· Wolborska model, and -- Yoon–Nelson model).

Pb^{2+} wastewater. The breakthrough curves reach saturation points (C_t/C_o = 0.95) at 142, 74, and 58 h, respectively, for 5, 10, and 15 cm^3/min flow rates. At these saturation times, the values of adsorption amounts (q_m) increased when the flow rate decreased, as shown in Table 1. Additionally, the value of height of the unused bed (H_{UNB}) for 5 mL/min was higher than those of 10 and 15 mL/min because the adsorption zone moved slowly at a low flow rate [35]. These results suggest that the low flow rate gives favorable adsorption of the Pb^{2+}.

Fig. 3 depicts breakthrough curves for different column adsorption experiments for column heights of 15, 20, and 30 cm. The column removal experiment was operated at constant flow rate of 10 cm^3/min. The Pb^{2+} concentration was 0.2 mM for permeation through the columns. Here, the composite fibers were packed, respectively, with 15, 20, and 30 g in each 15, 20, and 30 cm column. The results of Fig. 3 show that the values of C_t/C_o were increased to a saturation condition as well as Fig. 2. Results confirmed that the t_b and t_{st} for the Pb^{2+} elution from the packed column increased when a higher column height was used. For BV_b and q_m, a tendency was found by which a higher value was observed at higher column height. In addition, the values of H_{UNB} increased as column height increased, which indicated that the breakthrough curves became moderately flatter [36]. Increased column height caused longer EBRT. Therefore, increased column height can provide more retention time for better contact with the packed fibers. In addition, column adsorption tests of PES fiber having no zeolite were conducted as a reference experiment. The breakthrough curve for the reference fiber is depicted as green symbols in Fig. 3. As shown there, the breakthrough curve reached the saturation point of Pb^{2+} at 0.5 h. Consequently, it was apparent that the reference fiber had no removal capability for Pb^{2+}, meaning that the adsorption sites of Pb^{2+} were zeolites in the fibers.

Fig. 4 presents breakthrough curves for different Pb^{2+} concentration in the feed solution. Here, 20 g of the composite fiber was packed in 20 cm height column. Then, each Pb^{2+} feed solution was flowed into the column at a 10 cm^3/min flow rate. In the column permeation, the initial concentration of Pb^{2+} in the solutions was altered in the range of 0.05–0.2 mM concentration. It is noteworthy that the shape of the breakthrough curves became steeper for higher initial concentrations, meaning that the Pb^{2+} adsorption was rapidly saturated. Especially, Pb^{2+} detection at the column exit was confirmed at 2 h, when the initial concentration was 0.2 mM. Moreover, the values of BV_b and t_b apparently became small at high initial Pb^{2+} concentrations. This result demonstrated that the high Pb^{2+} concentration caused rapid elution of Pb^{2+}. As Table 1 shows, when the initial concentration increased from 0.05 to 0.1 mM, the values of q_m increased. Because slower diffusion of Pb^{2+} occurred at lower initial concentrations, slower saturation occurred with a shorter adsorption zone [36]. Therefore, the values of H_{UNB} decreased when the initial Pb^{2+} concentration decreased.

Fig. 5 portrays breakthrough curves of Pb^{2+} for various solution pH. Here, 20 g of the composite fiber was packed in 20 cm height column. Each Pb^{2+} feed solution was flowed into the column with a 10 cm^3/min flow rate. It was observed that C_t/C_o was 0.66 and 0.23 at 2 h for pH 2 and 3. Therefore, elution of Pb^{2+} occurred rapidly when the pH value in the solution was low. In addition, the values of t_{st} and q_m became smaller at lower pH. This result indicates that the solution pH affected the column adsorption performance to a considerable degree, and that composite fibers could only insufficiently absorb Pb^{2+} at low pH conditions. This insufficiency occurred because the positively charged Pb^{2+} was attracted to negatively charged ions by electrostatic interaction, but an excess amount of H_3O^+ in the lower pH solution led to competitive adsorption between Pb^{2+} ions and H_3O^+ to the zeolite sites [37]. A similar phenomenon was reported for our earlier study [25].

Results shown in Figs. 2–5 demonstrate that high column height, low flow rate, low initial Pb^{2+} concentration, and high solution pH in the column process were necessary for Pb^{2+} adsorption with sufficient contact time.

3.2. Consistency of dynamic adsorption models for the column adsorption process

As shown in Figs. 2–5 for the fitting of the resultant C_t/C_o data, experimental findings fit the Adams–Bohart model, Wolborska model, and Yoon–Nelson model. Three dynamic adsorption systems including these models were applied to fitting breakthrough curves. Only the Wolborska model was applied to the initial part of the breakthrough curves (until C_t/C_o = 0.5). Here, each calculated parameter and regression coefficient R^2 is presented in Table 2. Results show that the values of regression coefficient R^2 for the Adams–Bohart model were exactly same with those of the Yoon–Nelson: one for each condition. In addition, the R^2 values for both models were greater than 0.98, except for pH 2. This result indicated that both models well described the predicted curves of the breakthrough plots. As the predicted curve of Wolborska model in Figs. 2–5 shows, some column conditions including 15 mL/min, 15 cm, and 30 cm are apparently fitted better in initial parts of the curves (C_t/C_o = 0.3). However, application of Wolborska model shows a low value of R^2 relative to other models because the Wolborska model is based on the mass transfer for diffusion mechanisms in the range of the low concentration breakthrough curve [38]. For the Adams–Bohart model parameters at various flow rates, maximum adsorption capacity q_{AB} increased concomitantly with a decreasing flow rate, but the values of k_{AB} decreased. H_{UNB} increased concomitantly with an increasing flow rate. Therefore, the higher flow rate could cause faster mass transfer of the solute in the column and less Pb^{2+} adsorption to the composite fibers. A similar tendency was reported elsewhere in the literature [39]. In addition, in the case of column height, a tendency was found by which q_{AB} increased and k_{AB} decreased when the column height increased. The tendency was found to be dependent upon the flow rate. In the case of Adams–Bohart model parameters q_{AB} and k_{AB} for various initial concentrations,

Table 2
Calculated parameter of the Adams–Bohart model, Wolborska model, and Yoon–Nelson model

Adams–Bohart model	H (cm)	v (mL/h)	C_o (mmol/L)	pH	k_{AB} (L/mmol h)	N_o (mmol/L)	q_{AB} (mmol/g)	R^2
	20	5	0.2	5	0.225	89.00	0.279	0.9958
	20	10	0.2	5	0.349	85.20	0.268	0.9909
	20	15	0.2	5	0.420	77.56	0.244	0.9877
	30	10	0.2	5	0.234	84.04	0.264	0.9932
	15	10	0.2	5	0.355	82.99	0.261	0.9846
	20	10	0.15	5	0.282	98.22	0.308	0.9923
	20	10	0.1	5	0.279	108.2	0.340	0.9856
	20	10	0.05	5	0.465	106.1	0.333	0.9939
	20	10	0.2	3	0.343	36.82	0.1156	0.9884
	20	10	0.2	2	0.728	0	0	0.8811
Wolborska model	H (cm)	v (mL/h)	C_o (mmol/L)	pH	β (h^{-1})	N_o (mmol/L)	q_w (mmol/g)	R^2
	20	5	0.2	5	16.12	108.65	0.341	0.9642
	20	10	0.2	5	26.89	112.32	0.353	0.9812
	20	15	0.2	5	34.75	98.86	0.310	0.9325
	30	10	0.2	5	20.04	99.62	0.313	0.973
	15	10	0.2	5	30.97	104.17	0.327	0.9648
	20	10	0.15	5	26.31	128.58	0.404	0.9164
	20	10	0.1	5	28.06	138.58	0.435	0.9145
	20	10	0.05	5	39.21	127.43	0.400	0.9812
	20	10	0.2	3	13.89	71.13	0.223	0.9832
	20	10	0.2	2	–	–	–	–
Yoon–Nelson model	H (cm)	v (mL/h)	C_o (mmol/L)	pH	k_{YN} (h^{-1})	τ (h)	–	R^2
	20	5	0.2	5	0.045	90.05	–	0.9958
	20	10	0.2	5	0.070	44.61	–	0.9909
	20	15	0.2	5	0.084	27.08	–	0.9877
	30	10	0.2	5	0.047	66.00	–	0.9932
	15	10	0.2	5	0.071	32.59	–	0.9846
	20	10	0.15	5	0.041	68.19	–	0.9923
	20	10	0.1	5	0.028	113.18	–	0.9856
	20	10	0.05	5	0.023	222.13	–	0.9939
	20	10	0.2	3	0.068	19.28	–	0.9884
	20	10	0.2	2	0.093	0	–	0.8811

no clear tendency was observed when the values of k_{AB} differed. Also, q_{AB} decreased concomitantly with increasing initial concentration in the range of 0.1–0.2 mM as a result of insufficient residence time. For solutions with pH 2, 3, and 5, it was apparent that k_{AB} tended to increase as the solution pH decreased. In addition, q_{AB} showed lower values at lower pH, similarly to the tendency observed for q_m. Especially, q_{AB} was almost zero at pH 2.

3.3. Separation behavior observed in quaternary heavy metal ions for packed column containing the zeolite–polymer composite fiber

To study the adsorption behavior of heavy metals for the packed fiber system further, aqueous solutions having quaternary metal ions Pb^{2+}, Cd^{2+}, Cu^{2+}, and Ni^{2+} were used for separation by the composite fibers packed in the column. Here, the breakthrough curves of heavy metals were obtained as presented in Fig. 6. The composite fiber (20 g) was packed in a 20 cm height column. The quaternary ion solution containing each 0.05 mM concentration was flowed up into the column at 10 cm^3/min. Table 3 shows data for break time t_b, bed volume BV_b, saturation time t_{st}, height of unused bed H_{UNB}, and calculated q_m of each heavy metal. As Fig. 6 shows, the values of C_t/C_o in the breakthrough curves of Cd^{2+}, Cu^{2+}, and Ni^{2+} increased dramatically after 2 h. Among them, the

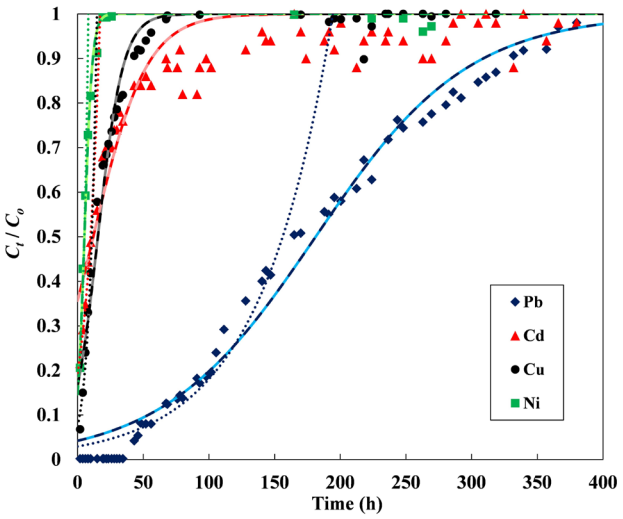

Fig. 6. Breakthrough curves of Pb^{2+}, Cd^{2+}, Cu^{2+}, and Ni^{2+} in quaternary mixed solution (— Adams–Bohart model, ··· Wolborska model, and -- Yoon–Nelson model).

Table 3
Calculated parameters of breakthrough curves in quaternary mixed heavy metal solutions

Heavy metals	C_o (mmol/L)	t_b (h)	BV_b	t_{st} (h)	H_{UNB} (cm)	q_m (mmol/g)
Pb^{2+}	0.05	67.5	1,131	366	16.3	0.263
Cd^{2+}	0.05	–	–	165	–	0.045
Cu^{2+}	0.05	–	–	72	–	0.017
Ni^{2+}	0.05	–	–	20	–	0.004

adsorption of Ni^{2+} reached saturation at 20 h, whereas the saturation times of Cu^{2+} and Cd^{2+} occurred, respectively, at 76 and 165 h. Comparison of Pb^{2+} with other ions showed that selective adsorption appeared on Pb^{2+} for the composite fibers. The leakage of Pb^{2+} in the elution solution was undetectable until 32 h at the exit portion of the column. The breakthrough curve showed that the Pb^{2+} ion concentration in the elution solution slowly rose after 43 h passed. It then reached saturation at 366 h. As presented in Table 3, the values of adsorption amount at saturation point q_m, for Pb^{2+}, Cd^{2+}, Cu^{2+}, and Ni^{2+} systems were, respectively, 0.263, 0.045, 0.017, and 0.004 mmol/g. The values of t_b, BV_b, and H_{UNB} were, respectively, 67.5 h; 1,131; and 16.3 cm for Pb^{2+}. Comparison of mixed and single Pb^{2+} solutions revealed that H_{UNB} for the mixed solution was longer than that for a single Pb^{2+} solution, implying that breakthrough curves of Pb^{2+} rose more moderately in mixed heavy metal solutions.

For the results of the quaternary metal ion tests, the Adams–Bohart model, Wolborska model, and Yoon–Nelson models were used for the breakthrough curves (Fig. 6). In addition, the calculated parameters for each model are represented in Table 4. The Adams–Bohart model and Yoon–Nelson model were fitted better for experimental breakthrough curves of Pb^{2+}, Cu^{2+}, and Ni^{2+} (Fig. 6). However, for the breakthrough curves of Cd^{2+}, R^2 values were lower than those of other heavy metals, and q_{AB} is lower than the experimental maximum adsorption capacity q_m. Both predicted curves of Cd^{2+} were saturated at 120 h, but the experimental breakthrough curve of Cd^{2+} rose rapidly until 80 h, and rose moderately thereafter until 300 h. As shown by the dotted line in Fig. 6, the Wolborska model well predicted experimental breakthrough model within C_t/C_o = about 0.2 and 0.6, respectively, for Pb^{2+} and other ions. However, the predicted curve deviates from the experimental data over that range.

Fig. 7 presents separation factors depending on the time for each heavy metal ion. Results show clearly that the values of separation factor for Pb^{2+} increased to about $\alpha = 300$ at 35 h. After 43 h, the separation factor decreased dramatically because the Pb^{2+} concentration in the eluted solution increased. Low separation factors were found for Cd^{2+}, Cu^{2+}, and Ni^{2+}: the composite fiber selectively retained Pb^{2+} in the mixed heavy metal solution, giving low selective adsorption ability of these ions for the composite fiber. In fact, the selectivity of Pb^{2+} was investigated under an excess K^+ condition in our earlier study, which indicated that a decreasing adsorption amount of Pb^{2+} became loose from a certain concentration of K^+. This phenomenon implies that adsorption of Pb^{2+} occurred both by ion exchange and the inclusion mechanism [25]. Therefore, selective adsorption of Pb^{2+} can occur in column adsorption for the reason demonstrated in our earlier study.

3.4. Regeneration and re-use study of composite fibers

To investigate the capability of regeneration and reuse of composite fibers, elution tests and re-using tests were conducted using acidic solutions. First, 20 g of composite fibers saturated with 0.2 mM Pb^{2+} were placed in 1.5 L of 0.1 M HNO_3 solution. After stirring for 48 h, the eluted Pb^{2+} concentration in the solutions was determined using AAS. The elution rate was calculated using the following equation.

Table 4
Calculated parameters of the Adams–Bohart model, Wolborska model, and Yoon–Nelson model for heavy metals (Pb^{2+}, Cd^{2+}, Cu^{2+}, and Ni^{2+})

		Heavy metal			
		Pb^{2+}	Cd^{2+}	Cu^{2+}	Ni^{2+}
Adams–Bohart model	k_{AB} (L/mmol h)	0.344	0.991	2.090	6.800
	N_o (mmol/L)	86.53	5.69	7.37	2.48
	q_{AB} (mmol/g)	0.272	0.018	0.023	0.008
	R^2	0.9834	0.8456	0.971	0.9354
Wolborska model	β (h^{-1})	33.68	15.64	24.72	17.96
	N_o (mmol/L)	92.84	8.18	7.03	3.91
	q_w (mmol/g)	0.292	0.026	0.022	0.012
	R^2	0.9324	0.9608	0.949	0.9062
Yoon– Nelson model	k_{YN} (h^{-1})	0.017	0.049	0.34	0.104
	τ (h)	181.22	11.98	15.43	5.19
	R^2	0.9834	0.8456	0.971	0.9354

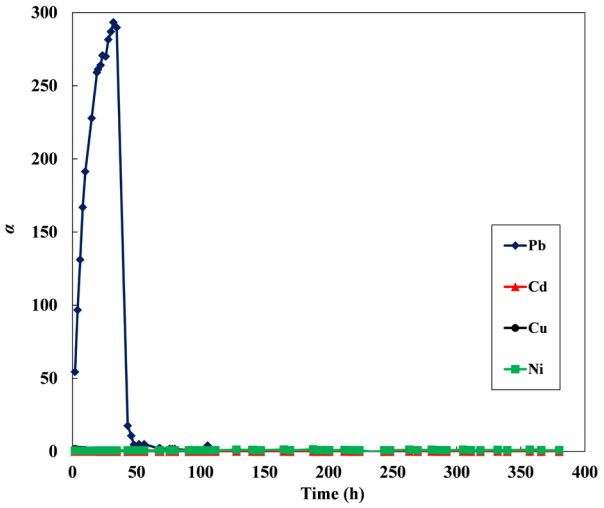

Fig. 7. Time dependence of separation factors of Pb^{2+}, Cd^{2+}, Cu^{2+}, and Ni^{2+} in quaternary mixed solutions at 0.05 mM concentration.

$$R = \frac{100VC_{el}}{qm} \tag{11}$$

Therein, R stands for the elution rate (%), C_{el} signifies the eluted Pb^{2+} concentration (mM), q denotes saturated adsorption amount (mmol/g), m expresses the mass of saturated adsorbent (g), and V stands for the solution volume (L). The obtained elution rate of lead ion for the composite fiber was about 9%, meaning that the Pb^{2+} adsorbing to the adsorbent was too tight to be eluted from the body. For re-use tests, the composite fibers treated with acidic solution were packed in the column again. Then 0.2 mM of Pb^{2+} solution flowed with 10 mL/min of flow rate. In the results, a high concentration of Pb^{2+} elution (C_t/C_o = 0.84) was confirmed at 2 h of the operation time. The composite fiber was again saturated by Pb^{2+} within 24 h. These results suggest that the regeneration and re-use of the present fiber was difficult, although the adsorbent was useful for stable immobilization of Pb^{2+} for practical use.

4. Conclusion

This report described a column study including zeolite–polymer composite fibers for parameters of different volumetric flow rates of aqueous Pb^{2+} solution. In addition, the column height, different Pb^{2+} initial concentration and solution pH were tested. Results demonstrated that the saturation time at lower flow rate lengthened beyond that of the lower flow rate. The saturation amounts of the Pb^{2+}, when the flow rate and the increase of column height caused increased saturation time and the column adsorption amount of Pb^{2+} to the fibers. These results underscore the importance of sufficient time to diffuse to access the binding sites of zeolites embedded in the composite fibers. For effective treatment, the composite fibers require sufficient residence time, even though the aqueous solution contained higher Pb^{2+} concentration. Regarding the adsorption models, the Adams–Bohart model and Yoon–Nelson model revealed better-fitted results. Additionally, it was observed that the Wolborska model fit well in the lower range of curves for some conditions. The column experiments in the quaternary metal ion for the mixture system suggest that the zeolite–polymer composite fibers exhibited predominant separation to Pb^{2+} ion. Consequently, the composite fibers had adsorption selectivity for Pb^{2+} in the continuous treatment by packed column composite fibers. In conclusion, the composite fibers had efficient ability of selective adsorption for Pb^{2+} ion in the column permeation and separation in the mixed solutions of heavy metal ions.

Acknowledgments

This study was supported by Kasai Corporation and the "Project to form a hub for human resources development and new industry creation".

Symbols

q_m	—	Saturation adsorption amount, mmol/g
C_t	—	Effluent heavy metal concentration, mM
C_o	—	Initial heavy metal concentration, mM
t	—	Time, h
v	—	Flow rate, cm^3/h
M	—	Mass of zeolite in packed composite fibers, g
t_b	—	Time at breakpoint ($C_t/C_o = 0.1$), h
t_{st}	—	Time at saturation point ($C_t/C_o = 0.95$), h
EBRT	—	Empty bed residence time, h
H	—	Column height, cm
π	—	Circle ratio
r	—	Column radius, cm
BV_b	—	Bed volume at breakpoint
V_o	—	Packing ratio of the fiber inside column, vol%
H_{UNB}	—	Height of unused bed, cm
α	—	Separation factor
Y_a and X_a	—	Mole fraction of feed and eluting solution
Y_b and X_b	—	Mole fraction of feed and eluting solution, respectively, for every metal ion excluding the target metal ion
k_{AB}	—	Kinetic constant of Adams–Bohart model, L/mmol h
N_o	—	Adsorption capacity per unit volume of the bed, mmol/L
L_v	—	Linear velocity, cm/h
q_{AB}	—	Maximum adsorption capacities calculated from Adams–Bohart model, mmol/g
β	—	Kinetics coefficient of the external mass transfer, h^{-1}
q_w	—	Maximum adsorption capacities calculated from Wolborska model, mmol/g
k_{YN}	—	Yoon–Nelson constant, h^{-1}
τ	—	Time at 0.5 of C_t/C_o, h
R	—	Elution rate, %
C_{el}	—	Eluted Pb^{2+} concentration, mM
m	—	Mass of saturated adsorbent, g
V	—	Solution volume, L

References

[1] K. Asaduzzaman, M.U. Khandaker, N.A. Binti Baharudin, Y.B.M. Amin, M.S. Farook, D.A. Bradley, O. Mahmoud, Heavy metals in human teeth dentine: a bio-indicator of metals exposure and environmental pollution, Chemosphere, 176 (2017) 221–230.

[2] A.P. Neal, T.R. Guilarte, Mechanisms of lead and manganese neurotoxicity, Toxicol. Res., 2 (2013) 99–114.

[3] World Health Organization, Guidelines for Drinking-Water Quality, 4th ed., World Health Organization, Geneva, 2011.

[4] A.M. Stefanowicz, M. Stanek, M.W. Woch, High concentrations of heavy metals in beech forest understory plants growing on waste heaps left by Zn-Pb ore mining, J. Geochem. Explor., 169 (2016) 157–162.

[5] H. Katsumata, S. Kaneco, K. Inomata, K. Itoh, K. Funasaka, K. Masuyama, T. Suzuki, K. Ohta, Removal of heavy metals in rinsing wastewater from plating factory by adsorption with economical viable materials, J. Environ. Manage., 69 (2003) 187–191.

[6] B. Bocca, A. Pino, A. Alimonti, G. Forte, Toxic metals contained in cosmetics: a status report, Regul. Toxicol. Pharmacol., 68 (2014) 447–467.

[7] L.T. Ogundele, O.K. Owoade, P.K. Hopke, F.S. Olise, Heavy metals in industrially emitted particulate matter in Ile-Ife, Nigeria, Environ. Res., 156 (2017) 320–325.

[8] S. Audry, J. Schäfer, G. Blanc, C. Bossy, G. Lavaux, Anthropogenic components of heavy metal (Cd, Zn, Cu, Pb) budgets in the Lot-Garonne fluvial system (France), Appl. Geochem., 19 (2004) 769–786.

[9] Z. Thong, G. Han, Y. Cui, J. Gao, T.-S. Chung, S.Y. Chan, S. Wei, Novel nanofiltration membranes consisting of a sulfonated pentablock copolymer rejection layer for heavy metal removal, Environ. Sci. Technol., 48 (2014) 13880–13887.

[10] M.M. Matlock, B.S. Howerton, D.A. Atwood, Chemical precipitation of lead from lead battery recycling plant wastewater, Ind. Eng. Chem. Res., 41 (2002) 1579–1582.

[11] A.P. Lim, A.Z. Aris, A review on economically adsorbents on heavy metals removal in water and wastewater, Rev. Environ. Sci. Biotechnol., 13 (2014) 163–181.

[12] A. Erto, L. Giraldo, A. Lancia, J.C. Moreno-Piraján, A comparison between a low-cost sorbent and an activated carbon for the adsorption of heavy metals from water, Water Air Soil Pollut., 224 (2013) 1531.

[13] R. Celis, M.C. HermosÍn, J. Cornejo, Heavy metal adsorption by functionalized clays, Environ. Sci. Technol., 34 (2000) 4593–4599.

[14] C. Zhang, Z. Yu, G. Zeng, B. Huang, H. Dong, J. Huang, Z. Yang, J. Wei, L. Hu, Q. Zhang, Phase transformation of crystalline iron oxides and their adsorption abilities for Pb and Cd, Chem. Eng. J., 284 (2016) 247–259.

[15] E. Da'na, Adsorption of heavy metals on functionalized-mesoporous silica: a review, Microporous Mesoporous Mater., 247 (2017) 145–157.

[16] E. Zanin, J. Scapinello, M. de Oliveira, C.L. Rambo, F. Franscescon, L. Freitas, J.M.M. de Mello, M.A. Fiori, J.V. Oliveira, J. Dal Magro, Adsorption of heavy metals from wastewater graphic industry using clinoptilolite zeolite as adsorbent, Process Saf. Environ. Protect., 105 (2017) 194–200.

[17] H. Sun, D. Wu, K. Liu, X. Guo, A. Navrotsky, Energetics of alkali and alkaline earth ion-exchanged zeolite A, J. Phys. Chem. C, 120 (2016) 15251–15256.

[18] M. Nielsen, R.Y. Brogaard, H. Falsig, P. Beato, O. Swang, S. Svelle, Kinetics of zeolite dealumination: insights from H-SSZ-13, ACS Catal., 5 (2015) 7131–7139.

[19] N.-Q. Feng, G.-F. Peng, Applications of natural zeolite to construction and building materials in China, Construct. Build. Mater., 19 (2005) 579–584.

[20] H. Li, W.-y. Shi, H.-b. Shao, M.-a. Shao, The remediation of the lead-polluted garden soil by natural zeolite, J. Hazard. Mater., 169 (2009) 1106–1111.

[21] A. Cincotti, A. Mameli, A.M. Locci, R. Orrù, G. Cao, Heavy Metals Uptake by sardinian natural zeolites: experiment and modeling, Ind. Eng. Chem. Res., 45 (2006) 1074–1084.

[22] L.A. Ciosek, K.G. Luk, Kinetic modelling of the removal of multiple heavy metallic ions from mine waste by natural zeolite sorption, Water, 9 (2017) 1–22.

[23] M. Król, A. Mikuła, Synthesis of the zeolite granulate for potential sorption application, Microporous Mesoporous Mater., 243 (2017) 201–205.

[24] T. Kobayashi, M. Ohshiro, K. Nakamoto, S. Uchida, Decontamination of extra-diluted radioactive cesium in Fukushima Water Using Zeolite–Polymer Composite fibers, Ind. Eng. Chem. Res., 55 (2016) 6996–7002.

[25] K. Nakamoto, M. Ohshiro, T. Kobayashi, Mordenite zeolite—polyethersulfone composite fibers developed for decontamination of heavy metal ions, J. Environ. Chem. Eng., 5 (2017) 513–525.

[26] T.K.K. Nakamoto, Fibrous mordenite zeolite - polymer composite adsorbents to methylene blue dye, Int. J. Eng. Tech. Res., 7 (2017) 131–136.

[27] E. Malkoc, Y. Nuhoglu, M. Dundar, Adsorption of chromium(VI) on pomace—an olive oil industry waste: batch and column studies, J. Hazard. Mater., 138 (2006) 142–151.

[28] G. Naja, B. Volesky, Behavior of the mass transfer zone in a biosorption column, Environ. Sci. Technol., 40 (2006) 3996–4003.

[29] M. Riazi, A.R. Keshtkar, M.A. Moosavian, Biosorption of Th(IV) in a fixed-bed column by Ca-pretreated *Cystoseira indica*, J. Environ. Chem. Eng., 4 (2016) 1890–1898.
[30] M.A.S.D. Barros, A.S. Zola, P.A. Arroyo, C.R.G. Tavares, E.F. Sousa-Aguiar, Chromium uptake from tricomponent solution in zeolite fixed bed, Adsorption, 12 (2006) 239–248.
[31] T.M. Darweesh, M.J. Ahmed, Batch and fixed bed adsorption of levofloxacin on granular activated carbon from date (*Phoenix dactylifera* L.) stones by KOH chemical activation, Environ. Toxicol. Pharmacol., 50 (2017) 159–166.
[32] G.S. Bohart, E.Q. Adams, Some aspects of the behavior of charcoal with respect to chlorine, J. Am. Chem. Soc., 42 (1920) 523–544.
[33] D. Sana, S. Jalila, A comparative study of adsorption and regeneration with different agricultural wastes as adsorbents for the removal of methylene blue from aqueous solution, Chin. J. Chem. Eng., 25 (2017) 1282–1287.
[34] Y.H. Yoon, J.H. Nelson, Application of gas adsorption kinetics I. A theoretical model for respirator cartridge service life, Am. Ind. Hyg. Assoc. J., 45 (1984) 509–516.
[35] S. Chatterjee, S. Mondal, S. De, Design and scaling up of fixed bed adsorption columns for lead removal by treated laterite, J. Clean. Prod., 177 (2018) 760–774.
[36] P.R. Rout, P. Bhunia, R.R. Dash, Evaluation of kinetic and statistical models for predicting breakthrough curves of phosphate removal using dolochar-packed columns, J. Water Process Eng., 17 (2017) 168–180.
[37] O.E. Abdel Salam, N.A. Reiad, M.M. ElShafei, A study of the removal characteristics of heavy metals from wastewater by low-cost adsorbents, J. Adv. Res., 2 (2011) 297–303.
[38] M. Lezehari, M. Baudu, O. Bouras, J.-P. Basly, Fixed-bed column studies of pentachlorophenol removal by use of alginate-encapsulated pillared clay microbeads, J. Colloid Interface Sci., 379 (2012) 101–106.
[39] T. Zang, Z. Cheng, L. Lu, Y. Jin, X. Xu, W. Ding, J. Qu, Removal of Cr(VI) by modified and immobilized *Auricularia auricula* spent substrate in a fixed-bed column, Ecol. Eng., 99 (2017) 358–365.